ELectronics EXpress

LETTER

IEICE Electronics Express, Vol.10, No.2, 1–12

A 60 GHz 3-dB tandem coupler using offset broadside-coupled lines on a silicon substrate

Hamid Kiumarsi[1a)], **Hiroyuki Ito**[1], **Kenichi Okada** [2], **Yusuke Uemichi**[3], **Yasuto Chiba**[3], **Noboru Ishihara**[1], **and Kazuya Masu**[1]

[1] *Solutions Research Laboratory, Tokyo Institute of Technology, 4259-S2-14 Nagatsuta, Midori-ku, Yokohama 226–8503, Japan*

[2] *Department of Physical Electronics, Tokyo Institute of Technology, Tokyo 152–8552, Japan*

[3] *Electron Device Laboratory, Fujikura Ltd., Sakura, Chiba, 285–8550, Japan*

a) *paper@lsi.pi.titech.ac.jp*

Abstract: In this letter, a 60 GHz tandem coupler using offset broadside-coupled lines is proposed on a silicon-based integrated passive device technology. Over the frequency band of 57–66 GHz, the measured insertion loss, amplitude imbalance, input return loss, isolation and phase error of the designed tandem coupler are better than 0.67 dB, 0.31 dB, 27.9 dB, 29.7 dB and 3.7° respectively. To the best of our knowledge the proposed coupler achieves the lowest reported insertion loss and amplitude imbalance for a 3-dB coupler on a silicon substrate at 60 GHz band. Furthermore using the even- and odd-mode analysis, the reason for a high directivity of edge-coupled lines and a low coupling level of broadside-coupled lines on the adopted technology is investigated and a solution for increasing the coupling level of broadside-coupled lines is proposed.

Keywords: 60 GHz band, tandem coupler, 3-dB coupler, broadside-coupled lines, quadrature, millimeter-wave passive devices

Classification: Microwave and millimeter wave devices, circuits, and systems

References

[1] C.-Y. Kuo, A. Y.-K. Chen, C.-M. Lee, and C.-H. Luo, "Miniature 60 GHz slow-wave CPW branch-line coupler using 90 nm digital CMOS process," *Electron. Lett.*, vol. 47, no. 16, pp. 924–925, Aug. 2011.

[2] I. Haroun, J. Wight, C. Plett, A. Fhaty, and D.-C. Chang, "Experimental analysis of a 60 GHz compact EC-CPW branch-Line coupler for mm-wave CMOS radios," *IEEE Microw. Wireless Compon. Lett.*, vol. 20, no. 4, pp. 211–213, April 2010.

[3] T.-Y. Chang, C.-L. Liao, and C. H. Chen, "Coplanar-waveguide tandem couplers with backside conductor," *IEEE Microw. Wireless Com-*

© IEICE 2013

DOI: 10.1587/elex.10.20120901
Received November 28, 2012
Accepted December 14, 2012
Published January 21, 2013

pon. Lett., vol. 13, no. 6, pp. 214–216, June 2003.
[4] J.-H. Cho, H.-Y. Hwang, and S.-W. Yun, "A design of wideband 3-dB coupler with N-section microstrip tandem structure," *IEEE Microw. Wireless Compon. Lett.*, vol. 15, no. 2, pp. 113–115, Feb. 2005.
[5] S.-W. Moon, M. Han, J.-H. Oh, J.-K. Rhee, and S.-D. Kim, "V-band CPW 3-dB tandem coupler using air-bridge structure," *IEEE Microw. Wireless Compon. Lett.*, vol. 16, no. 4, pp. 149–151, April 2006.
[6] T. H. Lee, *Planar Microwave Engineering*, Cambridge University Press, New York, 2004.
[7] R. Mongia, I. Bahl, and P. Bhartia, *RF and Microwave Coupled-Line Circuits*, Artech House, Boston, 1999.
[8] W. R. Eisenstadt and Y. Eo, "S-parameter-based IC interconnect transmission line characterization," *IEEE Trans. Compon., Hybrids, Manufact. Technol.*, vol. 15, no. 4, pp. 483–490, Aug. 1992.
[9] V. K. Tripathi, "Asymmetric coupled transmission lines in an inhomogeneous medium," *IEEE Trans. Microw. Theory Tech.*, vol. MTT-23, no. 9, pp. 734–739, Sept. 1975.
[10] D. M. Pozar, *Microwave Engineering*, 2nd ed., Wiley, New York, 2004.
[11] C. Nguyen, "Broadside-coupled coplanar waveguides and their end-Coupled band-pass filter applications," *IEEE Trans. Microw. Theory Tech.*, vol. 40, no. 12, pp. 2181–2189, Dec. 1992.
[12] C.-M. Tsai and K. C. Gupta, "A generalized model for coupled lines and its applications to two-layer planar circuits," *IEEE Trans. Microw. Theory Tech.*, vol. 40, no. 12, pp. 2190–2199, Dec. 1992.
[13] A. Tripathi and V. K. Tripathi, "A configuration-oriented SPICE model for multiconductor transmission lines in an inhomogeneous medium," *IEEE Trans. Microw. Theory Tech.*, vol. 46, no. 12, pp. 1997–2005, Dec. 1998.
[14] I. Haroun, C. Plett, Y.-C. Hsu, and D.-C. Chang, "Compact 60-GHz IPD-based branch-line coupler for system-on-package V-band radios," *IEEE Trans. Compon., Packag., Manuf. Technol.*, vol. 2, no. 7, pp. 1070–1074, July 2012.
[15] J. R. Reid and R. T. Webster, "A 60 GHz branch line coupler fabricated using integrated rectangular coaxial lines," *IEEE MTT-S Int. Microw. Symp. Dig.*, pp. 441–444, 2004.

1 Introduction

Although 3-dB quadrature couplers are key components in various microwave circuits, on-chip CMOS ones at 60 GHz suffer from a poor performance due to the conductive CMOS substrate and the absence of thick and wide lines. Examples of the such poor performances could be observed in [1, 2]. As shown in Fig. 1, in order to overcome the shortcomings of the CMOS technology for passive devices and yet to use its attractive features for active devices, we are considering a hybrid use of a CMOS chip and a passive chip integrating lower loss passive components for developing low-cost and high-performance millimeter-wave (MMW) systems. In this letter, in contrary to the previously reported tandem couplers in which *edge-coupled* lines were employed [3, 4, 5], a 60 GHz 3-dB tandem coupler using *offset broadside-coupled* lines is proposed and implemented on a silicon-based integrated passive de-

© IEICE 2013
DOI: 10.1587/elex.10.20120901
Received November 28, 2012
Accepted December 14, 2012
Published January 21, 2013

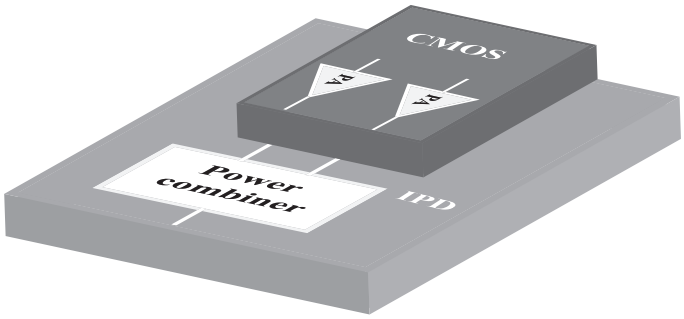

Fig. 1. The concept of a hybrid use of a CMOS chip and a passive chip.

vice (IPD) technology. Moreover a detailed analysis of coupled lines on our in-house IPD technology and a solution to increase the coupling level of broadside-coupled lines on the adopted technology is given.

2 The adopted silicon-based IPD technology

The cross-sectional view of the adopted silicon-based IPD technology is shown in Fig. 2 (a). In contrary to the conventional printed circuit boards (PCBs) in which making narrow line-width is difficult, the adopted IPD technology customized for MMW passives has a low cost silicon substrate as a mechanical backer which allows us to use a wafer process for fabrication and hence realizing a line-width as fine as 15 μm is possible.

As shown in Fig. 2 (a), this process has three metal layers, namely ground, 1st metal and top metal. It's noteworthy that employing a solid ground plane on the silicon substrate suppresses its loss; an option which is not available on the CMOS processes. Thickness of all metal layers formed by electroplating is 2 μm each and the thickness of dielectric layers with ϵ_r of 2.9 and loss tangent of 0.01, formed by coating a liquid resin are 10 μm each. Thus the total dielectric thickness is 20 μm and therefore a wider 50 Ω line (45 μm)

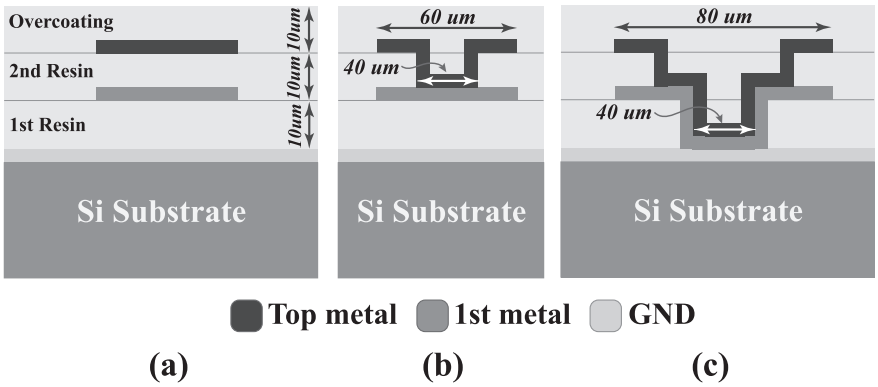

Fig. 2. The silicon-based IPD process used in this letter. (a) The cross-sectional view. (b) A via-hole for connecting the 1st metal to the top metal. (c) A stacked via-hole for connecting the top metal to the ground.

© IEICE 2013
DOI: 10.1587/elex.10.20120901
Received November 28, 2012
Accepted December 14, 2012
Published January 21, 2013

compared to those in the CMOS technology can be employed on the top metal. Having wider and thicker lines and suppressing the substrate loss by using a solid ground plane makes this process suitable for MMW passive devices.

Fig. 2 (b) shows a via-hole used for a connection between the 1st metal and the top metal and the one in Fig. 2 (c) depicts a stacked via-hole for connecting the top metal to the ground. These via-holes are quite big and a limiting factor for a designer. For example the via-hole in Fig. 2 (b) is too large to be used in a Lange coupler.

3 Edge-coupled and broadside-coupled lines

3.1 Edge-coupled lines

Full-wave EM (Electromagnetic) simulations using Agilent Momentum for edge-coupled lines on the top layer with the minimum line space of 15 μm show that the tightest achievable coupling level with acceptable RL (return loss) and isolation is -12.2 dB with line width of 20 μm which draws no interest for realizing of 3-dB couplers. However with line-width of 40 μm directivity of the coupler reaches the maximum of 57 dB while the coupling is -14 dB. Generally, edge-coupled lines on a PCB process tend to have a directivity as low as 10–15 dB in result of a different even- and odd-mode effective dielectric constants ($\epsilon_{eff,e}$ and $\epsilon_{eff,o}$ respectively). This is because fringing E fields above the substrate (through the air) in the odd-mode are much stronger than the even-mode, resulting in a lower $\epsilon_{eff,o}$ [6]. The achieved high directivity implies that the overcoating resin (see Fig. 2 (a)) in our process have partly solved the problem of inhomogeneous medium above and below the transmission line.

To extract the even- and odd-mode parameters, first four-port S-parameters got from a full-wave EM simulation are converted into a pair of two-port even- and odd-mode S-parameters using [7]

$$\begin{cases} S_{11e} = S_{22e} = S_{11} + S_{12} \\ S_{21e} = S_{12e} = S_{13} + S_{14} \\ S_{11o} = S_{22o} = S_{11} - S_{12} \\ S_{21o} = S_{12o} = S_{13} - S_{14} \end{cases} \tag{1}$$

where port numbering in Eq. (1) is depicted in Fig. 3. In the next step, $\epsilon_{eff,e}$ and $\epsilon_{eff,o}$ could be extracted by [8]

$$\begin{cases} K_{e(o)} = \sqrt{(1 + S_{11e(o)}^2 - S_{21e(o)}^2)^2 - (2S_{11e(o)})^2} \\ \gamma_{e(o)} = \left\{ ln\left(\frac{1 - S_{11e(o)}^2 + S_{21e(o)}^2 \pm K_{e(o)}}{2S_{21e(o)}} \right) / l \right\} \end{cases} \tag{2}$$

$$\epsilon_{eff,e(o)} = \left(\text{imag}(\gamma_{e(o)}) / k_0 \right)^2 \tag{3}$$

Where l is the length of the coupled lines, k_0 is the free-space wavenumber, and $\gamma_{e(o)}$ is the even-mode (odd-mode) propagation constant. Fig. 3 shows the simulated $\epsilon_{eff,e}$ and $\epsilon_{eff,o}$ of a pair of edge-coupled lines on the top metal

© IEICE 2013
DOI: 10.1587/elex.10.20120901
Received November 28, 2012
Accepted December 14, 2012
Published January 21, 2013

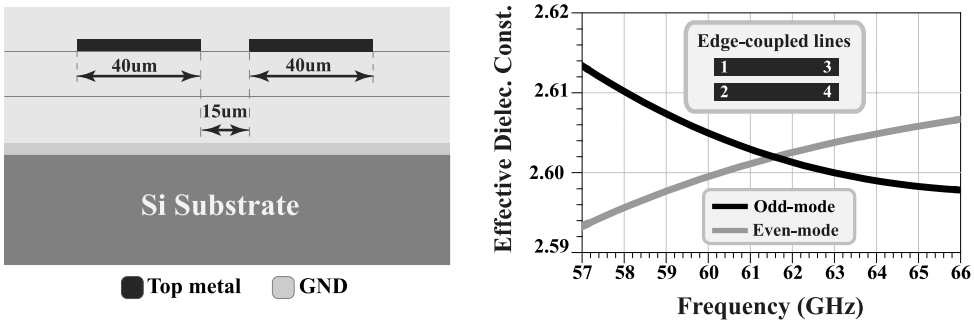

Fig. 3. Simulated even- and odd-mode effective dielectric constants of a pair of edge-coupled lines on the top metal with line-width of 40 μm and line space of 15 μm.

with a line-width of 40 μm and a line space of 15 μm. This very close $\epsilon_{eff,e}$ and $\epsilon_{eff,o}$ implies that edge-coupled lines on our silicon-based IPD technology could achieve a high directivity in contrary to their microstrip counterparts. Other simulations show that even if the line-width is changed from 40 μm, $\epsilon_{eff,e}$ and $\epsilon_{eff,o}$ will stay close to each other although they will not intersect as in Fig. 3.

3.2 Broadside-coupled lines

Although tighter couplers could be realized by broadside-coupled lines, the tightest one on this process barely reaches −5.4 dB of coupling. In order to investigate the cause of this low coupling level and possibly suggest a better structure for the current IPD process which can achieve higher coupling levels, an intuitive even- and odd-mode analysis is done.

The even/odd mode analysis is valid for coupled TEM lines in homogeneous medium or coupled identical lines in an inhomogeneous medium where an E-plane or H-plane could be placed in the symmetry plane of the coupler [9]. The broadside-coupled line is an asymmetric structure and even/odd modes cannot propagate independently, therefore the even/odd mode analysis is no more than an approximation in this case. Since in the current problem we are only interested in finding the reason and suggesting a better structure, an intuitive analysis is enough and there is no need for exact values. However the amount of introduced error should be quantified to judge whether the even/odd mode analysis is applicable in our intuitive analysis or not. In the following, we first analyze the broadside-coupled lines using eve/odd mode and then will prove later that the introduced error is tolerable in this case.

Recall that the coupling factor for a coupled line is [10]

$$C = \frac{Z_e - Z_o}{Z_e + Z_o} \tag{4}$$

where Z_e and Z_o are even- and odd-mode characteristic impedances. From Eq. (4), this low coupling level is a direct result of a smaller difference between even- and odd-mode characteristic impedances of broadside-coupled lines on

© IEICE 2013
DOI: 10.1587/elex.10.20120901
Received November 28, 2012
Accepted December 14, 2012
Published January 21, 2013

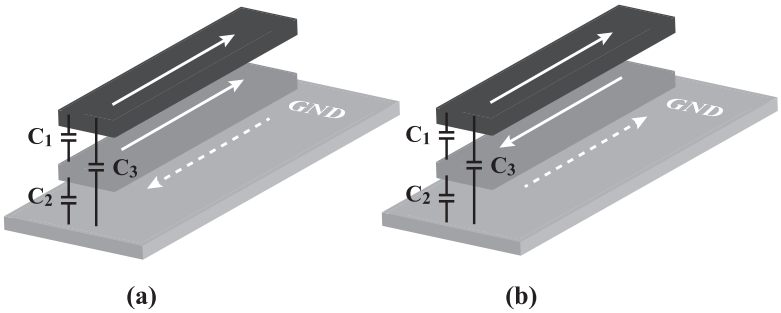

(a) (b)

Fig. 4. Excitations of a pair of broadside-coupled lines and relevant coupling capacitances and image currents (shown with dashed lines). (a) The even-mode. (b) The odd-mode.

the adopted technology. Since Z_e and Z_o could be given by

$$Z_{e(o)} = \sqrt{\frac{Le(o)}{Ce(o)}} \tag{5}$$

where $C_{e(o)}$ and $L_{e(o)}$ are the even-mode (odd-mode) capacitance and inductance per unit length of the coupled lines, we can focus on evaluating $C_{e(o)}$ and $L_{e(o)}$.

For an intuitive study, the even- and odd-mode excitations of the broadside-coupled lines along with their relevant coupling capacitors and image currents on the ground metal are considered in Fig. 4.

In the case of the even-mode shown in Fig. 4 (a), interline coupling capacitor of C_1 is open-circuited and C_2 has the largest contribution to the C_e, however in the odd-mode case in Fig. 4 (b), there is an imaginary ground plane through the midpoint of strip conductors (if the even/odd mode excitation is possible which is no more than an approximation) and C_1 can be considered as two $2C_1$ capacitors in series; therefore has a leading role in determining the C_o value. Direction of currents in Fig. 4 (a) and (b) indicate that the image current on the ground plane has a negative contribution to L_e and a positive contribution to L_o. This is because as it can be seen from Fig. 4 (a) for the even-mode, current on the lower strip conductor have a positive and image current on the ground plane has a negative mutual electromagnetic coupling to the upper strip conductor. Likewise for the odd-mode in Fig. 4 (b), current on the lower strip conductor have a negative and image current on the ground plane has a positive mutual electromagnetic coupling to the upper strip conductor.

If the 1st resin gets thicker, the image currents in Fig. 4 will get weaker resulting in a lower L_o and a higher L_e. However the increase rate is much higher in L_e than the decrease rate in L_o due to a stronger image current in the even-mode. Furthermore since C_e is mainly determined by C_2 and C_o by C_1 (C_1 is open-circuited in the even-mode), thicker 1st resin will result in a lower C_e, while C_o will not experience a noticeable change. Thus according to Eq. (5), Z_e will decrease while there will not be an obvious change in Z_o. Therefore for getting a greater separation between even- and odd-mode

© IEICE 2013
DOI: 10.1587/elex.10.20120901
Received November 28, 2012
Accepted December 14, 2012
Published January 21, 2013

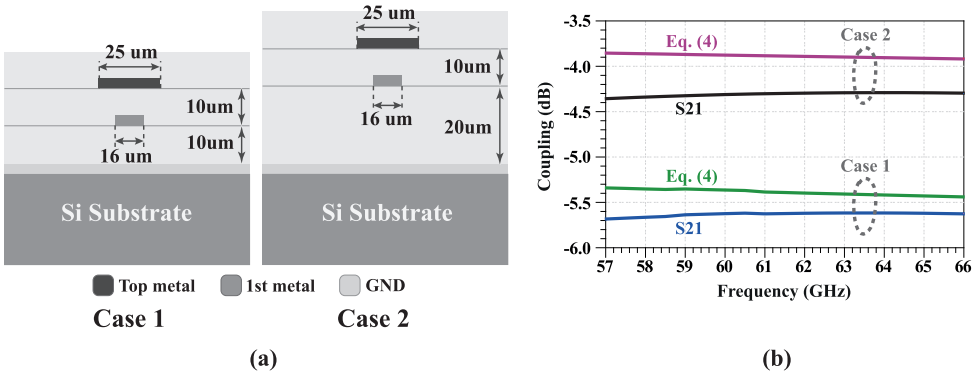

Fig. 5. (a) A broadside-coupled line on two different substrates and (b) it's simulated couplings.

Table I. Extracted even- and odd-mode parameters of Fig. 5 (a) at 61.5 GHz.

	C_e (pF)	C_o (pF)	L_e (nH)	L_o (nH)	Z_e (Ω)	Z_o (Ω)
Case 1	52.4	185.3	538.4	169.8	100.97	30.22
Case 2	39.6	1953.9	691.3	162.8	131.87	28.95

impedances which in turn translates to tighter broadside-coupled lines, *the 1st resin should be thicker than the 2nd resin.*

As shown in Fig. 5 (a), to verify the concept, a pair of broadside-coupled lines on the adopted substrate (case 1) and also on a substrate with a thicker 1st resin (case 2) were EM simulated using Agilent Momentum.

$C_{e(o)}$ and $L_{e(o)}$ could be obtained from standard transmission lines formulas [10].

$$C_{e(o)} = \text{imag}\left\{\frac{\gamma_{e(o)}}{Z_{e(o)} \cdot \omega}\right\} \tag{6}$$

$$L_{e(o)} = \text{imag}\left\{\frac{\gamma_{e(o)} \cdot Z_{e(o)}}{\omega}\right\} \tag{7}$$

The extracted even- and odd-mode parameters of the two cases in Fig. 5 (a) are given in Table I. Parameters in Table I clearly support the former qualitative discussion and suggest that for getting tight couplings (more separated Z_e and Z_o), 1st resin should be made thicker than the 2nd resin.

To see how much error is introduced, coupling with definition in Eq. (4) is compared with S21 (which is the real value of coupling) for case 1 and case 2 in Fig. 5 (b). Form this figure, the introduced error is about 6% in case 1 and 11% in case 2.

Asymmetric coupled lines (broadside-coupled lines belong to this category) should be characterized by two quasi-TEM propagation modes, that is, c-mode (in-phase) and π-mode (anti-phase). Parameters of interest are the ratios of voltages on conductor 2 to conductor 1 in c- and π-mode (R_c and R_π respectively), propagation constants (γ_c and γ_π) and line impedances

© IEICE 2013
DOI: 10.1587/elex.10.20120901
Received November 28, 2012
Accepted December 14, 2012
Published January 21, 2013

(Z_{c1}, Z_{c2}, $Z_{\pi1}$ and $Z_{\pi2}$) [9, 11, 12]. Note that the even/odd mode is a special case of c/π mode where $\gamma_c = \gamma_e$, $\gamma_\pi = \gamma_o$, $R_c = 1$ and $R_\pi = -1$. To assess the aforementioned even/odd mode analysis more rigorously, effective dielectric constants are compared. Noting that in the ideal case of a symmetric structure where the even/odd mode analysis is valid, $\epsilon_{eff,c} = \epsilon_{eff,e}$ and $\epsilon_{eff,\pi} = \epsilon_{eff,o}$ holds, the difference between these parameters could be a measure of introduced error by using even/odd mode analysis. Although c/π mode parameters can be readily derived from impedance or admittance matrix [12, 13], in this letter they are extracted from $ABCD$ matrix. To this end, first EM simulated four-port S-parameters are converted to the four-port $ABCD$ matrix using

$$\begin{bmatrix} A & B \\ C & D \end{bmatrix} = \begin{bmatrix} I - S11 & -Z_0(I + S11) \\ -S21 & -Z_0 S21 \end{bmatrix}^{-1} \begin{bmatrix} S12 & -Z_0 S12 \\ S22 - I & -Z_0(S22 + I) \end{bmatrix} \tag{8}$$

where all elements are 2×2 matrices and I is the 2×2 identity matrix. The Eq. (8) can be proved by writing definitions of $ABCD$ matrix and S-parameters. Then the c/π mode parameters can be extracted by

$$[A] = [M_V][\cosh(\gamma_i l)]_{diag}[M_V]^{-1} \tag{9}$$

$$[C] = [Y_{LM}] * [M_V][\sinh(\gamma_i l)]_{diag}[M_V]^{-1} \tag{10}$$

where γ_i is the ith mode propagation constant, that is, $\gamma_1 = \gamma_c$ and $\gamma_2 = \gamma_\pi$. $[Y_{LM}]$ is the line-mode admittance matrix whose element $Y_{LM_{km}}$ represents the characteristic admittance of the kth line for mth mode and l is the length of coupled lines. The operator "$*$" is the element-wise multiplication and $[M_V]$ is the voltage eigenvector matrix. $[M_V]$ and $[Y_{LM}]$ are defined by

$$[M_V] = \begin{bmatrix} 1 & 1 \\ R_c & R_\pi \end{bmatrix}, \quad [Y_{LM}] = \begin{bmatrix} Y_{c1} & Y_{\pi1} \\ Y_{c1} & Y_{\pi2} \end{bmatrix} \tag{11}$$

A simple eigen decomposition of matrix $[A]$ in Eq. (9) will give γ_c, γ_π, R_c and R_π. Then finding elements of $[Y_{LM}]$ from Eq. (10) is a straightforward task. Now $\epsilon_{eff,c}$ and $\epsilon_{eff,\pi}$ can be derived from

$$\epsilon_{eff,c(\pi)} = \left(imag(\gamma_{c(\pi)})/k_0\right)^2 \tag{12}$$

Fig. 6 shows the effective dielectric constants of even/odd modes and those of c/π modes for both case 1 and case 2. From this figure odd-mode has the highest error (with respect to the π-mode) which is about maximum of 13% for case 1 and maximum of 9% for case 2 whereas the even-mode (with respect to the c-mode) has about maximum of 3% for case 1 and maximum of 4% for case 2. Although results in Fig. 5 and Fig. 6 suggest that for a rigorous analysis, the studied broadside-coupled lines should be characterized by c- and π-mode, the introduced error is tolerable for an intuitive analysis. The thickness of 1st resin in case 2 can be adjusted to yield a 3-dB coupler. However this option is not available and the coupler should be designed based on case 1.

© IEICE 2013
DOI: 10.1587/elex.10.20120901
Received November 28, 2012
Accepted December 14, 2012
Published January 21, 2013

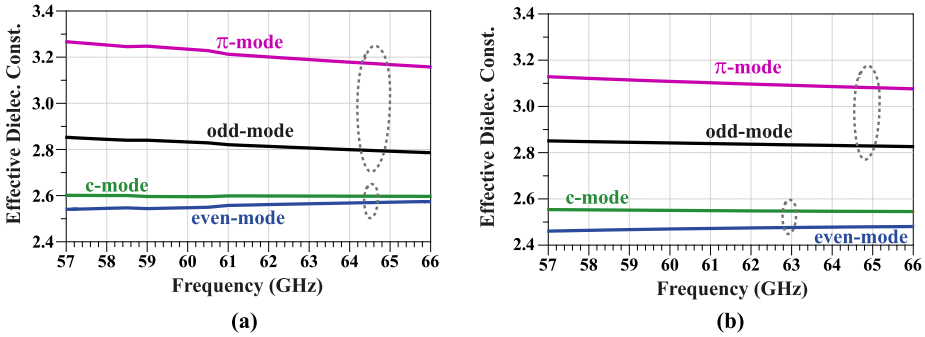

Fig. 6. The effective dielectric constants of even/odd modes and those of c/π modes for (a) case 1 and (b) case 2.

4 The designed MMW tandem coupler

4.1 Design

The analysis carried out in section 3 showed that using coupled lines is not a suitable choice for a 3-dB coupler in our process. When tight coupling is not possible, two loose coupled line couplers could be connected in a tandem configuration shown in Fig. 7 to yield a 3-dB coupler. Up until now most of the proposed tandem couplers were using two pairs of *edge-coupled* lines with a coupling level of 8.34 dB for each individual coupler [3, 4, 5]. Since, in the adopted process, edge-coupled lines are looser and broadside ones are tighter than 8.34 dB, *offset broadside-coupled* lines are used to achieve this goal. The final 3-dB coupler is optimized using Agilent Advanced Model Composer (AMC) for the best performance which eventually led to the layout shown in Fig. 8. To see the bandwidth of the designed tandem coupler, it's EM simulated S-parameters and phase difference over 10–110 GHz are shown in Fig. 9. As it's obvious from this figure, the designed coupler has a very wideband characteristics which is attributed to the inherent broadband property of broadside-coupled lines.

4.2 Measurement

Fig. 10 shows the micrograph of the fabricated 3-dB coupler occupying a core chip area of 0.288 mm^2. The EM simulated scattering parameters in

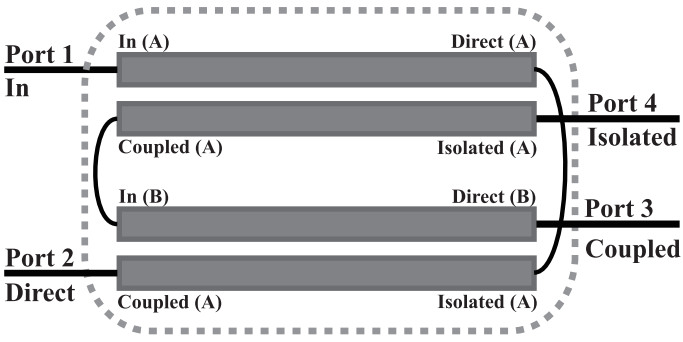

Fig. 7. The schematic representation of a typical tandem coupler.

© IEICE 2013
DOI: 10.1587/elex.10.20120901
Received November 28, 2012
Accepted December 14, 2012
Published January 21, 2013

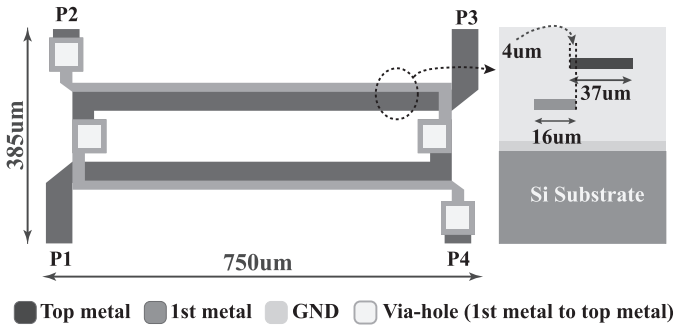

Fig. 8. The optimized layout of the designed tandem coupler.

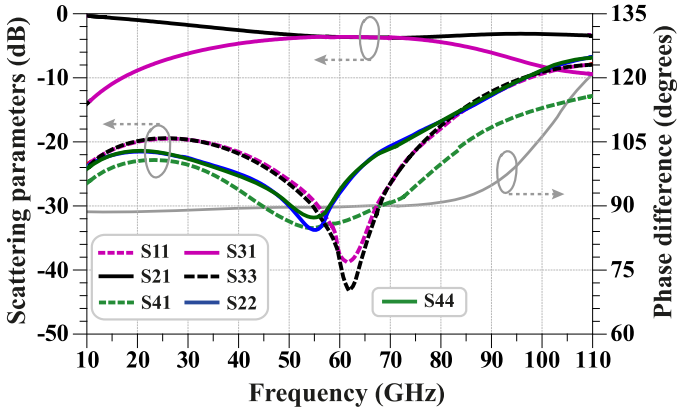

Fig. 9. The wideband simulated response of the designed tandem coupler.

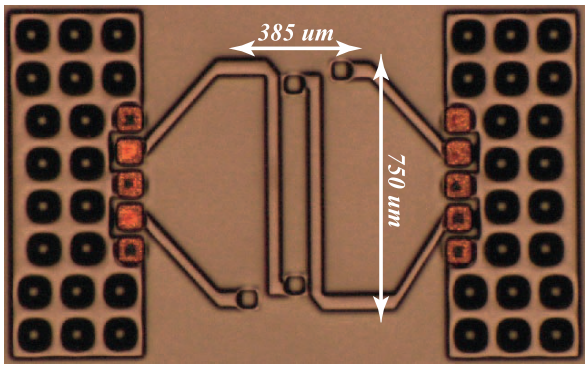

Fig. 10. The micrograph of the fabricated 60 GHz 3-dB tandem coupler.

the frequency range of 57–66 GHz are shown in Fig. 11 whereas the measured ones got by Agilent PNA-X Network Analyzer (N5247A) are shown in Fig. 12. The simulated and measured amplitude imbalances and phase differences are compared in Fig. 13. Discrepancies between the measured and simulated phase error (3.7° and 0.2° respectively) might be a result of a poor calibration of the measurement setup which is a hard task in the case of a full four-port calibration at the MMW frequencies. In an attempt to find the reason, a symmetric pair of transmission lines on the top metal was

© IEICE 2013
DOI: 10.1587/elex.10.20120901
Received November 28, 2012
Accepted December 14, 2012
Published January 21, 2013

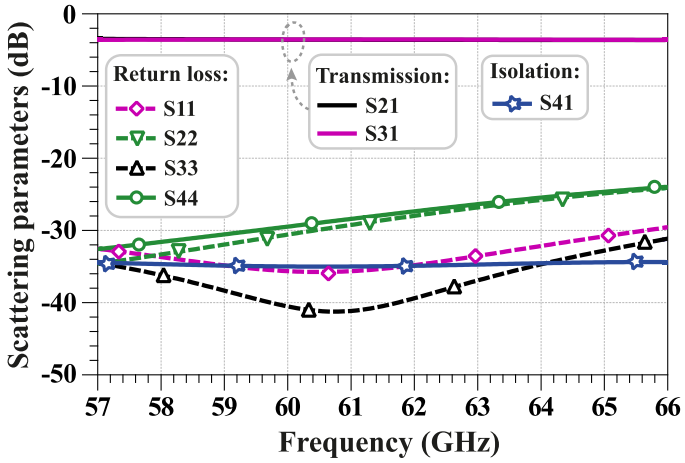

Fig. 11. The simulated scattering parameters of the tandem coupler.

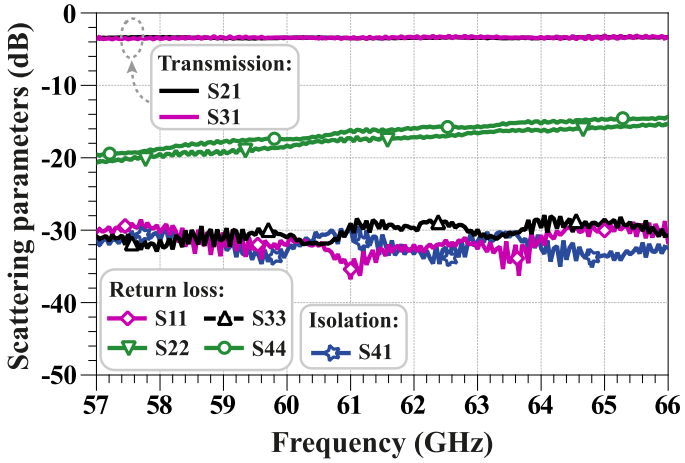

Fig. 12. The measured scattering parameters of the tandem coupler.

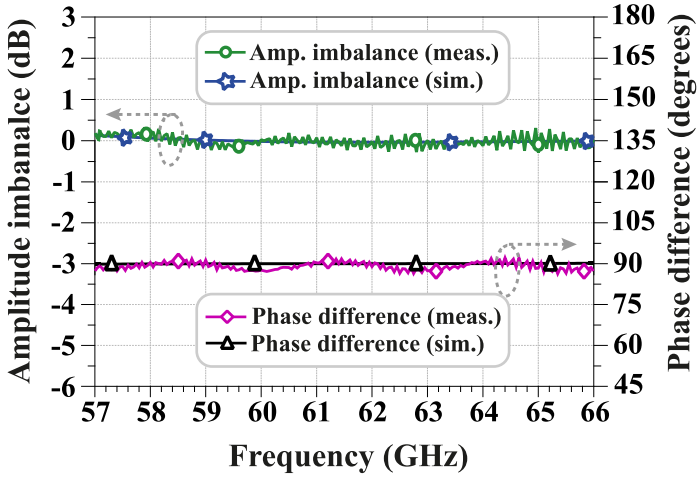

Fig. 13. The simulated and measured amplitude imbalance and phase difference of the tandem coupler.

© IEICE 2013
DOI: 10.1587/elex.10.20120901
Received November 28, 2012
Accepted December 14, 2012
Published January 21, 2013

Table II. Comparison of 60 GHz 3-dB quadrature couplers.

Ref.	BW (GHz)	Tech.	RL* (dB)	IL (dB)	Iso. (dB)	Phase error (°)	Amp. Imb. (dB)	Area (mm^2)
This work	**57–66**	**Silicon IPD**	**27.9**	**0.67**	**29.7**	**3.7**	**0.31**	**0.288**
[1]**	57–66	CMOS	17	4.5	19	8	2	0.083
[2]**			18	3	14	5.8	1	0.102
[14]**	57–64	Glass IPD	15	2	15	0.5	1.2	0.438
[15]	57–63	MEMS	18	1.1	18	4.37	0.55	1.58

*Denotes RL at the input port **The data is extracted from the available graphs.

measured and results showed almost the same discrepancies between simulated and measured results which clearly points to the poor calibration of the measurement setup. In Table II, the performance of the proposed coupler is compared to that of other reported MMW 3-dB quadrature couplers. Note that all the data in this table are the worst data at the specified frequency bandwidth (BW). From Table II, the proposed coupler shows a superior performance in terms of insertion loss (IL), amplitude imbalance and isolation compared with other reported ones in the 60 GHz band.

5 Conclusion

In this letter, a 60 GHz band tandem coupler using offset broadside-coupled lines is proposed on a silicon-based IPD technology. To the best of our knowledge the proposed coupler achieves the lowest reported insertion loss and amplitude imbalance for a 3-dB coupler on a silicon substrate. With its superior performance and lower cost compared to the CMOS counterparts, the proposed coupler is suitable for the low-cost and high-performance MMW systems.

Acknowledgments

This work was partly supported by the Global COE Program "Photonics Integration-Core Electronics", NEDO, KAKENHI, VDEC in collaboration with Agilent Technologies Japan Ltd., Cadence Design Systems Inc. and Mentor Graphics Inc.

© IEICE 2013
DOI: 10.1587/elex.10.20120901
Received November 28, 2012
Accepted December 14, 2012
Published January 21, 2013